Antigenic Characterization of Novel Human Norovirus GII.4 Variants San Francisco 2017 and Hong Kong 2019

Kentaro Tohma, Michael Landivar, Lauren A. Ford-Siltz,
Kelsey A. Pilewski, Joseph A. Kendra, Sandra Niendorf, Gabriel I. Parra

Norovirus is a major cause of acute gastroenteritis; GII.4 is the predominant strain in humans. Recently, 2 new GII.4 variants, Hong Kong 2019 and San Francisco 2017, were reported. Characterization using GII.4 monoclonal antibodies and serum demonstrated different antigenic profiles for the new variants compared with historical variants.

Norovirus is a major cause of acute gastroenteritis (*1*). Over past decades, variants of the predominant genotype, genotype 4 (GII.4), have continuously emerged to escape immunity (*2–5*). Since 2012, the Sydney 2012 variant has predominated worldwide (*6*). In 2019, GII.4 noroviruses that did not cluster with any known variants were reported circulating in different countries as early as 2016 (*7,8*). Based on phylogenetic clustering and number of mutations on major capsid viral proteins (VP1), the variant was classified GII.4 Hong Kong 2019 (*7*). The new variant caused no large outbreaks and did not eclipse the predominance of Sydney 2012. Another recently reported unique group of GII.4 noroviruses, the San Francisco 2017 variant, was retrospectively detected circulating during 2017–2022 (*9*). Both variants showed multiple mutations on major antigenic sites, including a single amino acid insertion next to the antigenic site A in San Francisco 2017 (*7,9,10*). We characterize the antigenicity of these 2 new variants using panels of GII.4 mouse monoclonal antibodies

(mAbs) and hyperimmune serum developed against historical GII.4 variants (*11,12*).

The Study

To determine the cross-reactivity of the 2 new variants with previously circulating variants, we produced virus-like particles (VLPs) for Hong Kong 2019 (GenBank accession no.: MN400355) and San Francisco 2017 (GenBank accession no. MW506849) viruses. We performed ELISA by using mAbs developed against Sydney 2012 virus (*11*) and the newly developed VLPs. Results demonstrated that the Hong Kong 2019 VLPs bound to most of the mAbs mapping to conserved sites from protruding (P) and shell (S) domains of the VP1, but only bound to 2/25 mAbs that mapped to variable antigenic sites and showed histo-blood group antigen (HBGA) blockade activity (Figure 1, panel A) (*11*). Those results were expected because mutational analyses showed that the Hong Kong 2019 viruses present multiple mutations on variable antigenic sites (Appendix, https://wwwnc.cdc.gov/EID/article/30/5/23-1694-App1.pdf) (*7*). The loss of binding of 3 cross-reactive mAbs that mapped to the P domain could be explained by unique mutations on the conserved sites (Appendix). VLPs from the San Francisco 2017 variant bound to all mAbs mapping to conserved sites of the VP1, but only to 4 mAbs that mapped to variable antigenic sites. Based on previous observations, alanine on positions 356, 359, or both, play a role in binding to mAbs 1C10 and 17A5 (*11*). Thus, alanine on those positions could explain the binding of mAbs to Hong Kong 2019 and San Francisco 2017 VLPs. Other mAbs mapping to the antigenic site G, 26E5 and 29A9, seem to require residues from antigenic site A (*11*). Mutations on antigenic site A in San Francisco 2017 could therefore result in loss of binding of these mAbs
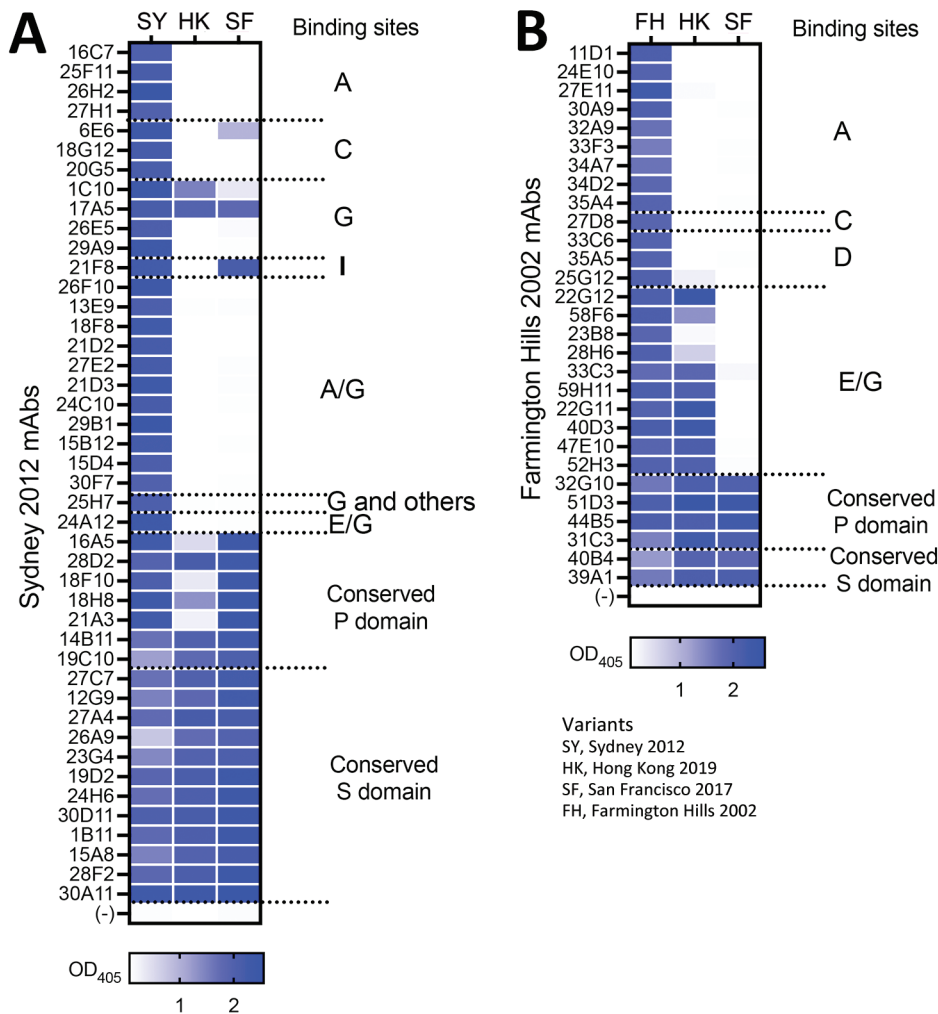
Figure 1. Monoclonal antibodies raised against 2 major GII.4 variants in a study of novel human norovirus GII.4 variants, San Francisco 2017 and Hong Kong 2019. A) Sydney 2012 mAb panel; B) Farmington Hills 2002 mAb panel. The heatmaps indicate ELISA binding strength (OD$_{405}$ values) of individual mAbs against virus-like particles from GII.4 Hong Kong 2019 and San Francisco 2017. Antibodies indicate minimal cross-reactivity between new and previously described variants. The binding sites of the mAbs were characterized in a previous study (*11*). mAbs, monoclonal antibodies; OD$_{405}$, optical density at 405 nm; P, protruding; S, shell.

regardless of similarity to antigenic site G on the Sydney 2012 variant. The 6E6 mAb, mapping to antigenic site C, was previously reported to cross-react weakly to Farmington Hills 2002 variant (*11*), which has 3 mutations compared with Sydney 2012. The San Francisco 2017 presented 4 mutations compared with Sydney 2012; the Hong Kong 2019 variant had 6 mutations on that site, explaining the differential binding of this mAb. Similarly, sequence differences on antigenic site I could explain the lack of binding of mAb 21F8 to Hong Kong 2019 VLPs.

Because Hong Kong 2019 and San Francisco 2017 present evolutionary convergence and share similar residues on several of the antigenic sites compared with the Farmington Hills 2002 variant (Appendix), we also tested those strains with mAbs developed against this ancestral variant (Figure 1, panel B). Both VLPs showed reactivity with all mAbs binding to conserved epitopes. As expected based on sequence similarity, Hong Kong 2019 showed reactivity only with mAbs mapping on antigenic site E/G. San

Francisco 2017 was negative to all mAbs mapping to variable sites, including antigenic site A, which presented only 3 mutations from Farmington Hills 2002 VLPs. Those data indicate that either a small number of changes are sufficient to abrogate binding of all 9 A-mapping mAbs or that the insertion near the antigenic site A has a major influence on the characteristics of this antigenic site.

To further characterize the antigenicity of these new variants, we tested the HBGA blocking activity of serum from mice immunized with VLPs from historical variants (Figure 2, panels A, B) (*12*), including the currently circulating Sydney 2012, the ancestral Farmington Hills 2002, and genetically or phylogenetically related variants: Osaka 2007 for Hong Kong 2019 viruses (*7*), and New Orleans 2009 and Apeldoorn 2007 for San Francisco 2017 viruses (*9*) (Appendix). The Hong Kong 2019 VLPs presented weak cross-blockade reactivity with the serum raised against all 3 viruses (mean 50% effective concentration = 118.5 for Sydney 2012,
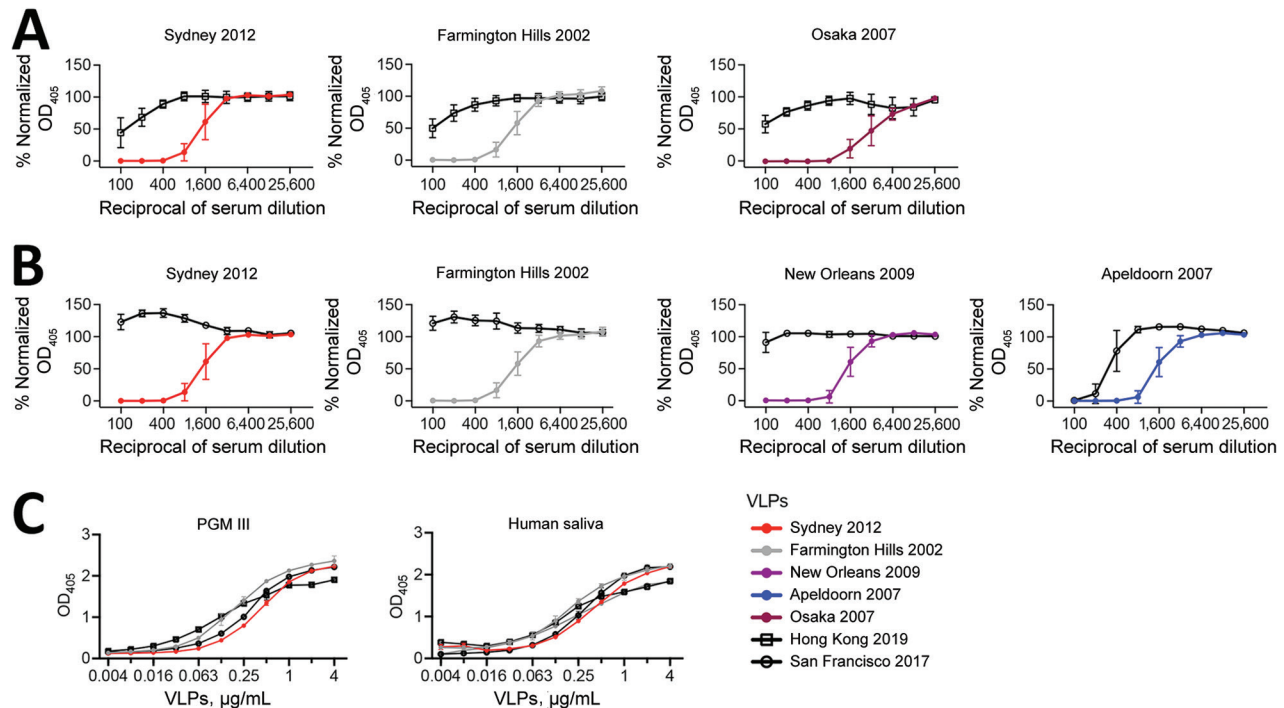
Figure 2. HBGA blockade and binding assays in a study of novel human norovirus GII.4 variants, San Francisco 2017 and Hong Kong 2019. A,B) Line graphs indicating normalized OD_{405} curves of GII.4 variants in HBGA blockade assays using mouse hyperimmune serum raised against currently circulating strains; A) Hong Kong 2019 VLPs against historical strains; B) San Francisco 2017 VLPs against historical strains. Normalized OD_{405} values were calculated by using values from positive and negative (serum only) control wells. C) OD_{405} curves of GII.4 variant VLPs in HGBA binding assays of Hong Kong 2019 and San Francisco 2017 VLPs and PGM III and human saliva, expressing the Lewis[a], Lewis[b], Lewis[y], H type-1, and H type-2 HBGA carbohydrates. PGM III was used as a source of HBGA carbohydrates. Human saliva was collected from a healthy adult volunteer under US Food and Drug Administration, Center for Biologics Evaluation and Research protocol no. CBER IRB 16–069B. HBGA, histo-blood group antigen; OD_{405}, optical density at 405 nm; PGM, porcine gastric mucin; VLP, virus-like particles.

116.9 for Farmington Hills 2002, and 87.6 for Osaka 2007 serum), with >12-fold differences compared with their homologous VLPs (Figure 2, panel A). That result was consistent with data from children with the fewest previous norovirus infections (*10*), supporting minimal cross-reactivity of Hong Kong 2019 to previous variants. In contrast, the San Francisco 2017 VLPs did not show cross-blockade reactivity with any of the serum samples tested from pandemic variants (Figure 2, panel B), including Sydney 2012 and Farmington Hills 2002, that shared similar sequences on the antigenic sites E/G (Sydney 2012) and A (Farmington Hills 2002) (Appendix). The only exception for cross-reactivity was with the serum raised against Apeldoorn 2007, which showed moderate cross-blockade activity with the San Francisco 2017 (50% effective concentration = 309.2, a 5-fold difference compared with homologous VLPs). Of note, GII.4 Apeldoorn 2007 and San Francisco 2017 share the same motif on the antigenic site D (Appendix). Thus, that cross-reactivity might be explained by antibodies mapping

on the antigenic site D from Apeldoorn 2007 variant.

Our data indicate that both Hong Kong 2019 and San Francisco 2017 variants present distinct antigenic profiles, yet both viruses have been circulating for >7 years without causing large outbreaks globally. Multiple examples of antigenically distinct noroviruses that spread worldwide without causing large outbreaks exist. Minor variants such as Osaka 2007 and Apeldoorn 2007 showed distinct antigenic profiles to variants that circulated before their emergence (*12*). Those variants caused local outbreaks and spread to multiple countries, but none predominated at the global level (*13*). Therefore, changes in antigenicity might not be the only factor determining the epidemic potential of noroviruses. Indeed, specific HBGA binding profiles were associated with emerging noroviruses (*14,15*). The new GII.4 variants bound to porcine gastric mucin III and human saliva, as did other current and archival variants (*9,10*) (Figure 2, panel C), suggesting that impairment of binding to HBGA did not cause the lower circulation of these viruses.

In conclusion, these 2 new norovirus variants are antigenically distinct from previously circulating variants. Whether these variants will predominate or are examples of the subdued circulation of minor norovirus variants remains to be determined. To prepare for future pandemics, we must delineate the factors that determine the overall fitness and predominance of GII.4 noroviruses, including but not limited to replication kinetics, pathogenicity, HBGA binding spectrum, and epidemiologic confounder.

About the Author

Dr. Tohma is a visiting associate at the Division of Viral Products, Food and Drug Administration, Silver Spring, Maryland, USA. His research interests include viral genetic and antigenic evolution, epidemiology, and norovirus vaccine design.

References

1. Lopman BA, Steele D, Kirkwood CD, Parashar UD. The vast and varied global burden of norovirus: prospects for prevention and control. PLoS Med. 2016;13:e1001999. PubMed https://doi.org/10.1371/journal.pmed.1001999
2. Lindesmith LC, Costantini V, Swanstrom J, Debbink K, Donaldson EF, Vinjé J, et al. Emergence of a norovirus GII.4 strain correlates with changes in evolving blockade epitopes. J Virol. 2013;87:2803–13. https://doi.org/10.1128/JVI.03106-12
3. Lindesmith LC, Donaldson EF, Lobue AD, Cannon JL, Zheng DP, Vinje J, et al. Mechanisms of GII.4 norovirus persistence in human populations. PLoS Med. 2008;5:e31. https://doi.org/10.1371/journal.pmed.0050031
4. Siebenga JJ, Lemey P, Kosakovsky Pond SL, Rambaut A, Vennema H, Koopmans M. Phylodynamic reconstruction reveals norovirus GII.4 epidemic expansions and their molecular determinants. PLoS Pathog. 2010;6:e1000884. https://doi.org/10.1371/journal.ppat.1000884
5. Tohma K, Lepore CJ, Gao Y, Ford-Siltz LA, Parra GI. Population genomics of GII.4 noroviruses reveal complex diversification and new antigenic sites involved in the emergence of pandemic strains. mBio. 2019;10:10. https://doi.org/10.1128/mBio.02202-19
6. Parra GI, Tohma K, Ford-Siltz LA, Eguino P, Kendra JA, Pilewski KA, et al. Minimal antigenic evolution after a decade of norovirus GII.4 Sydney_2012 circulation in humans. J Virol. 2023;97:e0171622. https://doi.org/10.1128/jvi.01716-22
7. Chan MC, Roy S, Bonifacio J, Zhang LY, Chhabra P, Chan JCM, et al.; for NOROPATROL2. Detection of norovirus variant GII.4 Hong Kong in Asia and Europe, 2017–2019. Emerg Infect Dis. 2021;27:289–93. https://doi.org/10.3201/eid2701.203351
8. Chuchaona W, Chansaenroj J, Puenpa J, Khongwichit S, Korkong S, Vongpunsawad S, et al. Human norovirus GII.4 Hong Kong variant shares common ancestry with GII.4 Osaka and emerged in Thailand in 2016. PLoS One. 2021;16:e0256572. https://doi.org/10.1371/journal.pone.0256572
9. Chhabra P, Tully DC, Mans J, Niendorf S, Barclay L, Cannon JL, et al. Emergence of novel norovirus GII.4 variant. Emerg Infect Dis. 2023;30:163–7.
10. Lindesmith LC, Boshier FAT, Brewer-Jensen PD, Roy S, Costantini V, Mallory ML, et al. Immune imprinting drives human norovirus potential for global spread. mBio. 2022;13:e0186122. https://doi.org/10.1128/mbio.01861-22
11. Tohma K, Ford-Siltz LA, Kendra JA, Parra GI. Dynamic immunodominance hierarchy of neutralizing antibody responses to evolving GII.4 noroviruses. Cell Rep. 2022;39:110689. https://doi.org/10.1016/j.celrep.2022.110689
12. Kendra JA, Tohma K, Ford-Siltz LA, Lepore CJ, Parra GI. Antigenic cartography reveals complexities of genetic determinants that lead to antigenic differences among pandemic GII.4 noroviruses. Proc Natl Acad Sci U S A. 2021;118:e2015874118. https://doi.org/10.1073/pnas.2015874118
13. Kendra JA, Tohma K, Parra GI. Global and regional circulation trends of norovirus genotypes and recombinants, 1995–2019: a comprehensive review of sequences from public databases. Rev Med Virol. 2022;32:e2354. https://doi.org/10.1002/rmv.2354
14. Shanker S, Choi JM, Sankaran B, Atmar RL, Estes MK, Prasad BV. Structural analysis of histo-blood group antigen binding specificity in a norovirus GII.4 epidemic variant: implications for epochal evolution. J Virol. 2011;85:8635–45. https://doi.org/10.1128/JVI.00848-11
15. Zhang XF, Huang Q, Long Y, Jiang X, Zhang T, Tan M, et al. An outbreak caused by GII.17 norovirus with a wide spectrum of HBGA-associated susceptibility. Sci Rep. 2015;5:17687. https://doi.org/10.1038/srep17687

Address for correspondence: Kentaro Tohma, Center for Biologics Evaluation and Research, US Food and Drug Administration, 10903 New Hampshire Ave, Bldg 52/72, Rm 1376, Silver Spring, MD 20993, USA; email: kentaro.tohma@fda.hhs.gov

Antigenic Characterization of Novel Human Norovirus GII.4 Variants, San Francisco 2017 and Hong Kong 2019

Appendix

Genetic Analyses

The emergence of GII.4 variants was associated with multiple mutations mapping to five major antigenic sites (namely, A, C, D, E, and G) on the major capsid protein, VP1 (*1,2*). These antigenic sites are involved in viral neutralization and blockade of interactions between the VP1 and histo-blood group antigen (HBGA) carbohydrates (*3*), which are ligands that facilitate norovirus infection (*4–7*). This Appendix provides a comprehensive mutational analysis of new GII.4 variants using a large, n = 3,142, dataset of complete GII.4 VP1 sequences (*8*), and the viruses classified as GII.4 Hong Kong 2019 (*9*) and GII.4 San Francisco 2017 (*10*). The phylogenetic relationship of new and historical GII.4 variants were estimated using maximum-likelihood method using VP1 amino acid sequences. In the phylogenetic analysis, the dataset was downsized to consist of randomly subsampled sequences with a maximum of 30 sequences per variant. The phylogenetic tree was calculated using the best-fit substitution model as implemented in IQ-TREE (*11*). The number of nucleotide or amino acid changes between previous GII.4 variants and new variants was measured using *phylotools* and *utils* packages and consensus sequence from each variant was estimated using *seqinr* package in R (*12*).

As indicated in previous studies (*9,10*), the phylogenetic tree showed that Hong Kong 2019 and San Francisco 2017 variants are distinct from other GII.4 variants (Appendix Figure 1). The Hong Kong 2019 is most closely related to the Osaka 2007 variant, while San Francisco 2017 branched out from Sydney 2012 variants. The mutational analysis of the new variants confirmed multiple substitutions on the major antigenic sites A, C, D, E, and G as indicated in previous studies (*9,10,13*), and on other subdominant sites, namely I, resulting in different amino

acid sequence patterns (Appendix Figures 2, 3). Hong Kong 2019 showed unique patterns on antigenic sites A, D, I, and multiple other positions on the P domain. As expected by the phylogenetic analysis (*9*) (Appendix Figure 1), this virus showed sequence similarities with Osaka 2007 on the major antigenic sites. Notably, Hong Kong 2019 displayed the same amino acid sequence on antigenic site E from the ancestral Farmington Hills 2002, but the overall difference between these two viruses is marked by ≥4 amino acid changes on each of the other four (A, C, D, G) antigenic sites (Appendix Figure 2).

In addition to an insertion described between positions 293 and 294 (*10*), the San Francisco 2017 variant contained multiple amino acid mutations on antigenic site A as compared with Sydney 2012 (median: 3 mutations out of 8 residues) and Apeldoorn 2007 (median: 4 mutations), but ≤2 mutations on antigenic sites D, E, and G (Appendix Figure 2). Interestingly, San Francisco 2017 presented large intra-variant variations on antigenic site A, and 6 out of 15 San Francisco 2017 strains reported in previous study (*10*) shared same sequence on this antigenic site with Sydney 2012 viruses that were detected in late 2010s and 2020s (*8*). These late Sydney 2012 viruses showed evolutionary convergence into the ancestral GII.4 variants on antigenic site A (*8*) (Appendix Figure 4). Likewise, San Francisco 2017 presented a similar antigenic site A (median: 3 mutations) to ancestral Grimsby 1995 or Farmington Hills 2002 variants, but a completely different antigenic site G (median: ≥5 mutations out of 6 residues) (Appendix Figure 2). Although these variants shared similarity on antigenic site A, their consensus nucleotide sequences indicated a large divergence between them. Thus, the San Francisco 2017 consensus sequence displayed 5–7 nucleotide but only 2 amino acid changes as compared to the Farmington Hills 2002 and Grimsby 1995 consensus sequences of antigenic site A (Appendix Figure 4). When comparing the nucleotide sequence of these codon positions with phylogenetically closer variants (Apeldoorn 2007, early and late Sydney 2012 viruses), the San Francisco 2017 viruses presented 4–6 nucleotide changes that resulted in 2–4 amino acid mutations. Of note, consensus San Francisco 2017 presented a different codon pattern on position 368 (GAA) as compared with Farmington Hills 2002 (AAC) and Grimsby 1995 (ACC), which is same codon (GAA) with early and late Sydney 2012 viruses. Together, these data suggest that the San Francisco 2017 variant converged into similar amino acids on the antigenic site A present in the ancestral variants via different evolutionary pathways, confirming previous

observations that there are constraints on the use of residues throughout the evolution of GII.4 norovirus (*8*).

In conclusion, the new variants presented multiple amino acid changes on the major antigenic sites when compared with all previously described viruses, with several of them converging into motifs observed in previous variants. A description of effect of these mutations on the antigenic profile of these variants is presented in the main text.

References

1. Tohma K, Lepore CJ, Gao Y, Ford-Siltz LA, Parra GI. Population genomics of GII.4 noroviruses reveal complex diversification and new antigenic sites involved in the emergence of pandemic strains. mBio. 2019;10:10. PubMed https://doi.org/10.1128/mBio.02202-19

2. Lindesmith LC, Costantini V, Swanstrom J, Debbink K, Donaldson EF, Vinje J, et al. Emergence of a norovirus GII.4 strain correlates with changes in evolving blockade epitopes. J Virol. 2013;87:2803–13. PubMed https://doi.org/10.1128/JVI.03106-12

3. Tohma K, Ford-Siltz LA, Kendra JA, Parra GI. Dynamic immunodominance hierarchy of neutralizing antibody responses to evolving GII.4 noroviruses. Cell Rep. 2022;39:110689. PubMed https://doi.org/10.1016/j.celrep.2022.110689

4. Haga K, Ettayebi K, Tenge VR, Karandikar UC, Lewis MA, Lin SC, et al. Genetic manipulation of human intestinal enteroids demonstrates the necessity of a functional fucosyltransferase 2 gene for secretor-dependent human norovirus infection. mBio. 2020;11:e00251-20.

5. Marionneau S, Ruvoen N, Le Moullac-Vaidye B, Clement M, Cailleau-Thomas A, Ruiz-Palacois G, et al. Norwalk virus binds to histo-blood group antigens present on gastroduodenal epithelial cells of secretor individuals. Gastroenterology. 2002;122:1967–77.

6. Tan M, Huang P, Meller J, Zhong W, Farkas T, Jiang X. Mutations within the P2 domain of norovirus capsid affect binding to human histo-blood group antigens: evidence for a binding pocket. J Virol. 2003;77:12562–71. PubMed https://doi.org/10.1128/JVI.77.23.12562-12571.2003

7. Rockx BHG, Vennema H, Hoebe CJPA, Duizer E, Koopmans MPG. Association of histo-blood group antigens and susceptibility to norovirus infections. J Infect Dis. 2005;191:749–54. https://doi.org/10.1086/427779

8. Parra GI, Tohma K, Ford-Siltz LA, Eguino P, Kendra JA, Pilewski KA, et al. Minimal antigenic evolution after a decade of norovirus GII.4 Sydney_2012 circulation in humans. J Virol. 2023;97:e0171622. PubMed https://doi.org/10.1128/jvi.01716-22

9. Chan MC, Roy S, Bonifacio J, Zhang LY, Chhabra P, Chan JCM, et al.; for NOROPATROL2. Detection of norovirus variant GII.4 Hong Kong in Asia and Europe, 2017–2019. Emerg Infect Dis. 2021;27:289–93. PubMed https://doi.org/10.3201/eid2701.203351

10. Chhabra P, Tully DC, Mans J, Niendorf S, Barclay L, Cannon JL, et al. Emergence of novel norovirus GII.4 variant. Emerg Infect Dis. 2024;30:163–7. PubMed https://doi.org/10.3201/eid3001.231003

11. Trifinopoulos J, Nguyen LT, von Haeseler A, Minh BQ. W-IQ-TREE: a fast online phylogenetic tool for maximum likelihood analysis. Nucleic Acids Res. 2016;44(W1):W232–5.

12. R Core Team. R: a language and environment for statistical computing. Vienna, Austria: R Foundation for Statistical Computing; 2023.

13. Lindesmith LC, Boshier FAT, Brewer-Jensen PD, Roy S, Costantini V, Mallory ML, et al. Immune imprinting drives human norovirus potential for global spread. mBio. 2022;13:e0186122. PubMed https://doi.org/10.1128/mbio.01861-22

14. Kendra JA, Tohma K, Ford-Siltz LA, Lepore CJ, Parra GI. Antigenic cartography reveals complexities of genetic determinants that lead to antigenic differences among pandemic GII.4 noroviruses. Proc Natl Acad Sci U S A. 2021;118:e2015874118. PubMed https://doi.org/10.1073/pnas.2015874118
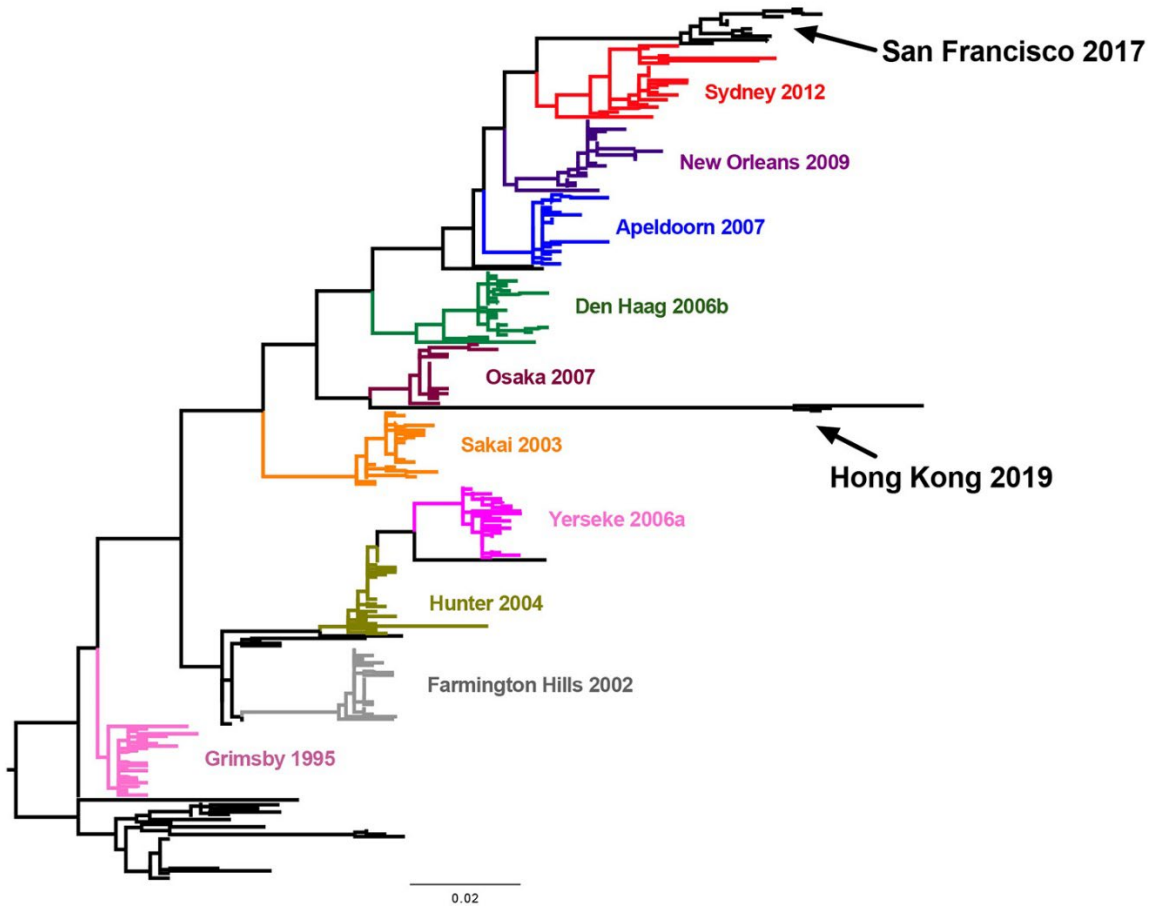
Appendix Figure 1. Phylogenetic tree showing the evolutionary relationship of the new variants, GII.4 Hong Kong 2019 and San Francisco 2017, with previously described GII.4 variants. The phylogenetic tree was calculated with the maximum-likelihood method and randomly sampled (n = 338) VP1 sequences with sequences from new variants, Hong Kong 2019 and San Francisco 2017. Scale bar indicates the genetic distance, measured by the number of amino acid substitutions per site.
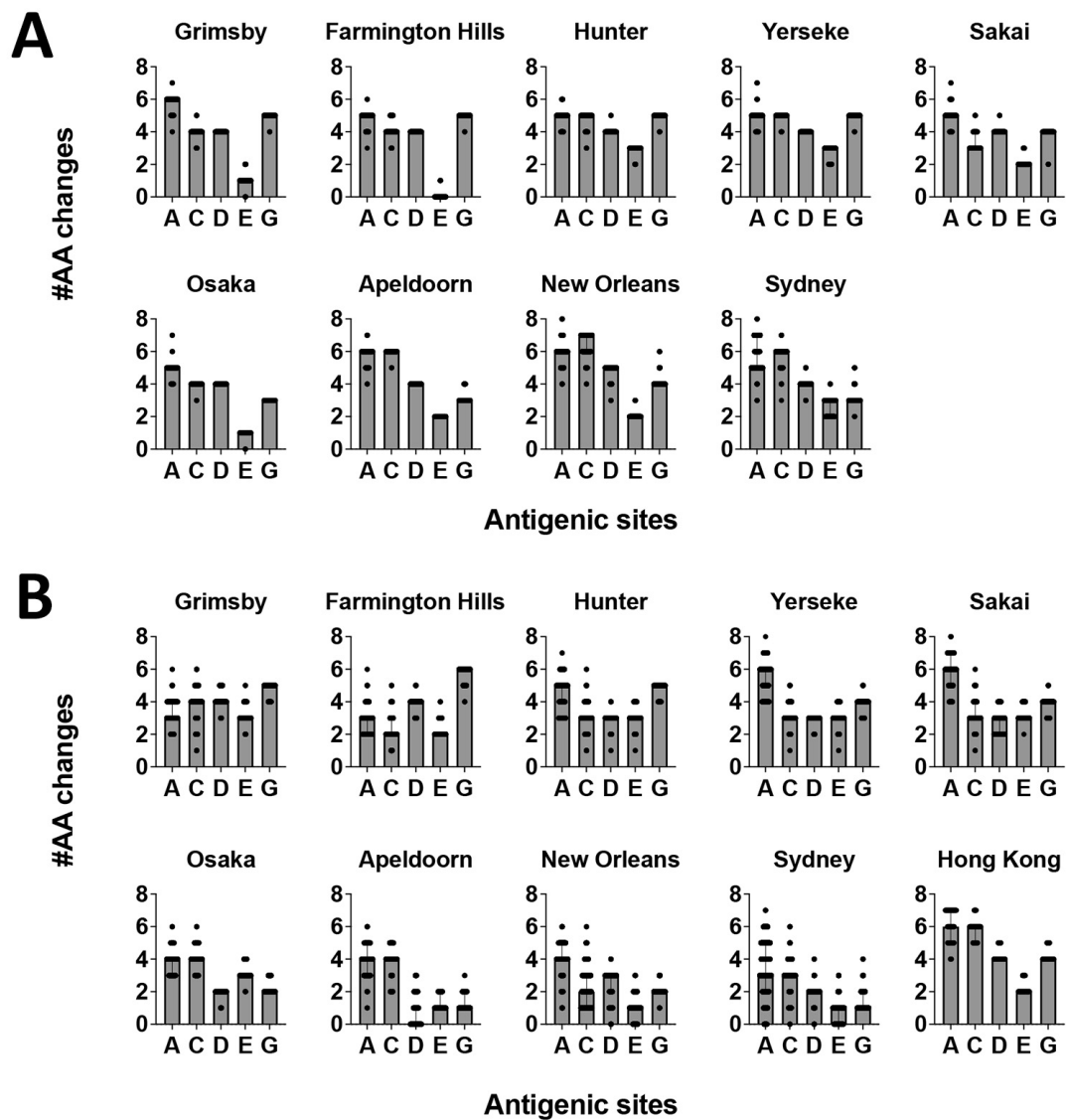
Appendix Figure 2. Number of amino acid mutations on individual major antigenic sites between new and previous variants. The bar graphs show the number of amino acid mutations on each antigenic site between Hong Kong 2019 (A) or San Francisco 2017 (B) and historical GII.4 variants (n = 3,142). The bar and error bars indicate median and interquartile range. AA, amino acid.

Major antigenic sites involved in HBGA-blockade and neutralization — pre-A, A, C

Variant	Strain (accession number)	pre-A 292	293	Insertion	A 294	295	296	297	298	368	372	373	C 339	340	341	375	376	377	378
Hong Kong	CUHK-NS-2200/Hong Kong/2019 (MN400355)	H	I	-	A	G	T	R	Q	G	E	D	K	G	D	L	Q	S	G
San Francisco	561/Gabon/2018 (MW506849)	Q	T	A	A	G	T	H	N	A	T	N	R	G	N	L	E	T	N
Sydney	RockvilleD1/United States/2012 (KY424328)	H	I	-	T	G	S	R	N	E	D	H	R	T	D	F	E	A	N
New Orleans	Virginia/Unites States/2010 (KX353958)	H	I	-	P	G	S	R	N	A	D	N	R	T	N	F	E	T	N
Apeldoorn	Iwate4/Japan/2008 (AB541274)	H	I	-	T	G	S	R	N	A	D	N	R	A	D	F	D	A	N
Osaka	Osaka/Japan/2007 (AB434770)	H	I	-	A	G	S	R	N	A	D	N	R	S	D	F	E	S	G
Farmington Hills	MD-2004/United States/2004 (DQ658413)	H	I	-	A	D	T	H	N	N	N	N	R	G	D	F	E	T	G
Farmington Hills	Oxford/United Kingdom/2003 (AY588022)	H	I	-	A	G	T	H	N	N	N	N	R	G	D	F	E	T	G

Major antigenic sites involved in HBGA-blockade and neutralization — D, E, G; Subdominant I

Variant	Strain (accession number)	D 393	394	395	396	397	E 407	411	412	413	414	352	355	356	357	359	364	I 250	255	504
Hong Kong	CUHK-NS-2200/Hong Kong/2019 (MN400355)	E	N	P	H	F	S	R	T	G	H	S	A	A	D	A	N	Y	T	P
San Francisco	561/Gabon/2018 (MW506849)	D	T	A	H	R	S	R	N	T	P	Y	S	N	D	A	R	F	S	Q
Sydney	RockvilleD1/United States/2012 (KY424328)	S	T	T	H	R	S	R	N	T	H	Y	S	A	D	A	R	F	S	Q
New Orleans	Virginia/Unites States/2010 (KX353958)	S	A	T	P	R	S	R	N	I	H	Y	S	A	D	S	R	F	S	Q
Apeldoorn	Iwate4/Japan/2008 (AB541274)	D	T	A	H	R	S	R	N	S	H	Y	S	A	D	A	R	F	S	Q
Osaka	Osaka/Japan/2007 (AB434770)	S	T	T	H	R	N	R	T	G	H	L	S	A	D	A	R	Y	S	Q
Farmington Hills	MD-2004/United States/2004 (DQ658413)	N	G	T	H	Q	S	R	T	G	H	S	D	V	H	T	S	F	G	Q
Farmington Hills	Oxford/United Kingdom/2003 (AY588022)	N	G	T	H	Q	S	R	T	G	H	S	D	V	H	T	S	F	G	Q

Other sites with mutations specific to the new variants — Shell, Protruding

Variant	Strain (accession number)	Shell 144	256	289	290	299	302	331	348	350	362	366	379	386	398	409	438	447	449	471	508
Hong Kong	CUHK-NS-2200/Hong Kong/2019 (MN400355)	V	A	D	L	F	H	Q	K	I	S	R	T	I	S	T	M	L	I	D	A
San Francisco	561/Gabon/2018 (MW506849)	I	T	S	V	Y	N	R	L	T	L	Q	Q	V	N	S	L	M	L	E	V
Sydney	RockvilleD1/United States/2012 (KY424328)	I	A	D	V	Y	N	Q	K	T	L	Q	Q	V	N	S	M	M	L	D	V
New Orleans	Virginia/Unites States/2010 (KX353958)	I	A	D	V	Y	N	Q	K	T	L	Q	Q	V	N	S	M	M	L	D	V
Apeldoorn	Iwate4/Japan/2008 (AB541274)	I	A	D	V	Y	N	Q	K	T	L	Q	Q	V	N	S	M	M	L	D	V
Osaka	Osaka/Japan/2007 (AB434770)	I	A	D	V	Y	N	Q	K	T	L	Q	Q	V	N	S	M	M	L	D	V
Farmington Hills	MD-2004/United States/2004 (DQ658413)	I	A	D	V	Y	N	Q	K	T	L	Q	Q	V	N	S	M	M	L	D	V
Farmington Hills	Oxford/United Kingdom/2003 (AY588022)	I	A	D	V	Y	N	Q	K	T	L	Q	Q	V	N	S	M	M	L	D	V

Residues: Acidic; Basic; Polar neutral; Hydrophobic; Proline; Glycine; Cysteine

Appendix Figure 3. Sequence alignment of major strain(s) from GII.4 variants used in immunoassays in this study. VLPs from the MD-2004/United States/2004 and RockvilleD1/United States/2012 viruses were used to generate mouse monoclonal antibodies (mAbs) (*3*). VLPs from Oxford/United Kingdom/2002, Osaka/Japan/2007, Iwate4/Japan/2008, Virginia/Unites States/2010, and RockvilleD1/United States/2012 were used to generate mouse hyperimmune sera (*14*). Because MD-2004/Unites States/2004 virus, which was used to produce mAbs for the Farmington Hills 2002 variant, has a mutation (G295D) on antigenic site A, sera raised against Oxford/United Kingdom/2003 was selected to test responses at the polyclonal level. Individual cells are colored based on the biochemical properties of the residues. HGBA, histo-blood group antigen; VLPs, virus-like particles.

Amino acid position	294			295			296			297			298			368			372			373			# Differences to San Francisco 2017	
Nucleotide position	880	881	882	883	884	885	886	887	888	889	890	891	892	893	894	1102	1103	1104	1114	1115	1116	1117	1118	1119	Nucleotide	Amino acid
San Francisco 2017 — *A* *G* *S* *H* *N* *E* *N* *N*	G	C	A	G	G	T	A	G	T	C	A	T	A	A	C	G	A	A	A	A	C	A	A	C		
Late Sydney 2012 (2018-2022) — *T* *G* *S* *H* *N* *E* *N* *H*	**A**	C	A	G	G	T	A	G	T	C	A	**C**	A	A	C	G	A	A	A	A	C	**C**	A	**T**	4	2
Early Sydney 2012 (2012-2017) — *T* *G* *S* *R* *N* *E* *D* *H*	**A**	C	A	G	G	T	A	G	T	C	**G**	T	A	A	C	G	A	A	**G**	A	C	**C**	A	**T**	5	4
Apeldoorn 2007 — *T* *G* *S* *R* *N* *A* *D* *N*	**A**	C	A	G	G	T	A	G	T	C	**G**	T	A	A	C	G	**C**	**C**	**G**	A	C	A	A	**T**	6	4
Farmington Hills 2002 — *A* *G* *T* *H* *N* *N* *N* *N*	G	C	A	G	G	T	A	**C**	T	C	A	T	A	A	**T**	**A**	A	**C**	A	A	C	A	A	**T**	5	2
Grimsby 1995 — *A* *G* *S* *H* *D* *T* *N* *N*	G	C	A	G	G	**C**	A	G	T	C	A	T	**G**	A	**T**	**A**	**C**	**C**	A	A	C	A	A	**T**	7	2

Appendix Figure 4. Comparison of consensus codon and amino acid sequences of antigenic site A from GII.4 variants. The amino acid sequences are shown in italic on the top and the corresponding codon (nucleotide) sequences are shown on the bottom. Mutations as compared to San Francisco 2017 consensus sequences are highlighted in bold and red.